2011 American Control Conference
on O'Farrell Street, San Francisco, CA, USA
June 29 - July 01, 2011

Global TCF Based Contouring Controller Design for an Industrial Biaxial Precision Gantry With Accurate Parameter Estimations

Chuxiong Hu, Bin Yao and Qingfeng Wang

Abstract— **This paper presents a global task coordinate frame (TCF) based integrated direct/indirect adaptive robust contouring controller (DIARC) for an industrial biaxial gantry that achieves not only excellent contouring performance but also accurate parameter estimations. Contouring control problem is first formulated in a recently proposed global task coordinate frame where the calculation of the contouring error is rather accurate and not affected by the curvature of the desired contour. A physical model based indirect type parameter estimation algorithm is then synthesized to obtain accurate on-line estimates of unknown physical model parameters. An integrated direct/indirect adaptive robust contouring controller with dynamic compensation type fast adaptation is also constructed to preserve the excellent transient and steady-state contouring performance of the direct adaptive robust control (DARC) designs. Comparative experimental results obtained on a high-speed industrial biaxial precision gantry show that the proposed algorithm not only achieves the best contouring performance but also has accurate physical parameter estimations.**

I. INTRODUCTION

During contouring tasks, lacking coordination of axes can significantly contribute to contouring errors which are the ultimate performance evaluation for coordinated motion of multi-axes systems [1], [2], [3]. To solve this problem, Koren [4] first proposed the cross-coupled control strategy to strengthen the coordination of axes. Later on, the contouring control problem is formulated in a task coordinate frame (TCF) by using either the concept of generalized curvilinear coordinates in [5], or the locally defined coordinates attached to the desired contour in [6]. Under the task coordinate formulation, a control law could be designed to assign different dynamics to the normal and tangential directions relative to the desired contour. This formulation has been used in a number of recent publications [1], [7]. However, the presented control techniques cannot explicitly deal with parametric uncertainties and uncertain nonlinearities.

In [8], [9], the adaptive robust control (ARC) strategy in [10], [11] and the local TCF approach in [6] have been integrated to develop contouring controllers for high-speed biaxial linear-motor-driven gantries under both parametric uncertainties and uncertain nonlinearities. Though sufficient for some applications, they are not well suited for applications demanding not only good output tracking performance but also accurate on-line parameter estimations for secondary purposes such as machine component health monitoring and prognosis. Accurate parameter estimations are also achieved in our previous work [12], but the TCF used is locally defined based on the desired trajectory to be tracked on the desired contour, which is valid only for applications with very small actual tracking errors and small curvatures.

This paper focuses on applications having large curvatures and demanding stringent contouring control performance as well as accurate real-time estimates of physical parameters. Specifically, to address the problems associated with the locally defined task coordinate frame (LTCF) based contouring controllers [8], [12] for large curvatures, our recently developed orthogonal global task coordinate frame (GTCF) [13] will be used. The presented GTCF is globally defined and has nothing to do with the specific desired trajectory to be tracked on the contour. Furthermore, the calculation of the contouring error is rather accurate and not affected by the curvature of the desired contour. The integrated direct/indirect adaptive robust control (DIARC) scheme [14] is then employed to construct a coordinated motion controller for a biaxial gantry to achieve not only excellent contouring performance but also accurate on-line parameter estimations. Comparative experimental results obtained on a linear motors driven high-speed industrial biaxial precision gantry verify that the proposed global TCF based DIARC controller not only achieves the best contouring performance but also reasonably accurate parameter estimations in practical applications.

II. PROBLEM FORMULATION

A. Orthogonal Global Task Coordinate Frame (TCF)

Traditionally, the TCF for a biaxial system is locally defined at the desired position $P_d(x_d(t), y_d(t))$ based on the desired trajectory given by $\mathbf{q_d}(t) = [x_d(t), y_d(t)]^T$. Such a definition depend on not only the geometry of the desired contour but also the desired motion. As such, when the actual tracking error is large or the actual position differs from the desired point $\mathbf{q_d}(t)$ significantly, the calculated contouring error could be far different from the actual one as illustrated in Fig.1 by the coordinate frame in dashed lines. Intuitively, the actual contouring error depends on the geometry of the desired contour and the actual path of the system only and should have no relation with the desired motion. To overcome this problem, in [13], an orthogonal global TCF is introduced

The work is supported in part by the US National Science Foundation (Grant No. CMMI-1052872), the National Basic Research and Development Program of China (973 Program. Grant No. 2007CB714000) and the Ministry of Education of China through a Chang Jiang Chair Professorship.

Chuxiong Hu (fyfox.hu@gmail.com), a PhD candidate, and Qingfeng Wang (qfwang@zju.edu.cn), a professor, are with the State Key Laboratory of Fluid Power Transmission and Control, Zhejiang University, Hangzhou 310027, China. Chuxiong Hu is also with the State Key Laboratory of Tribology, Department of Precision Instruments and Mechanology, Tsinghua University, Beijing 100084, China.

Bin Yao is a Professor of School of Mechanical Engineering at Purdue University, West Lafayette, IN 47907, USA (byao@purdue.edu). He is also a Chang Jiang Chair Professor at the State Key Laboratory of Fluid Power Transmission and Control of Zhejiang University.

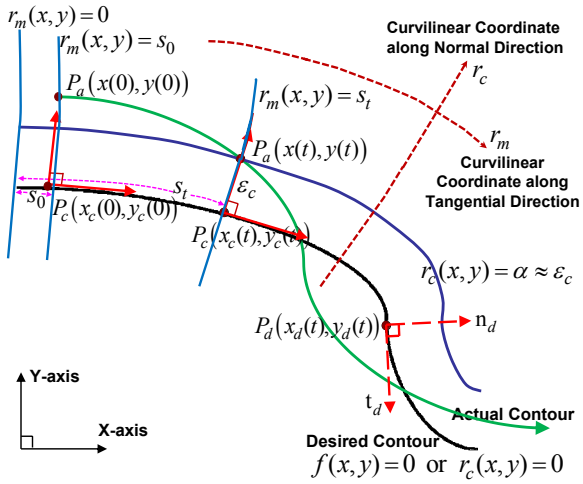

Fig. 1. A globally defined orthogonal task coordinate frame.

solely based on the geometry of the desired contour defined by $f(x,y)=0$ where x and y denote the coordinates of the biaxial gantry system and f is a known smooth function as shown in Fig.1. Specifically, a curvilinear coordinate along the normal direction of the desired contour can be defined as

$$r_c(x,y)=\frac{f(x,y)}{\sqrt{{f_x}^2+{f_y}^2}} \tag{1}$$

where $f_x=\frac{\partial f}{\partial x}$ and $f_y=\frac{\partial f}{\partial y}$. With this curvilinear coordinate, the desired contour can be simply described by constraining it to zero in the global TCF, i.e., $r_c(x,y)=0$, and the normal direction of the desired contour is aligned with the direction of this curvilinear coordinate. Furthermore, it is shown in [13] that the coordinate value of the actual position along this curvilinear coordinate direction, i.e., $r_c(x(t),y(t))$ where $(x(t),y(t))$ represents the Cartesian coordinates of the actual position at time t, is essentially the same as the actual contouring error ε_c, the distance between the actual position $P_a(x(t),y(t))$ and $P_c(x_c(t),y_c(t))$, the projection of $P_a(x(t),y(t))$ onto the desired contour along its normal direction as illustrated in Fig.1.

With the above definition of the curvilinear coordinate representing the contouring error, the other curvilinear coordinate $r_m(x,y)$ is defined based on the curve length on the desired contour between the reference point and the projection of the position (x,y) at the desired contour along its normal direction, e.g., the curve lengths s_0 and s_t shown in Fig.1 for the initial position $P_a(x(0),y(0))$ and the actual position $P_a(x(t),y(t))$ respectively. The details are given in [13]. Overall, the proposed task coordinate system is defined by the following curvilinear coordinate transformation:

$$\mathbf{r}=\mathbf{h}(\mathbf{q})=\begin{bmatrix} r_c(x,y) \\ r_m(x,y) \end{bmatrix} \tag{2}$$

It is shown in [13] that, on the desired contour, the directional vector along the coordinate r_c, $[\frac{\partial r_c}{\partial x},\frac{\partial r_c}{\partial y}]^T$, is the same as the unit vector along the normal direction of the desired contour, $[\frac{f_x}{\sqrt{f_x^2+f_y^2}},\frac{f_y}{\sqrt{f_x^2+f_y^2}}]^T$, and the directional vector along the coordinate r_m, $[\frac{\partial r_m}{\partial x},\frac{\partial r_m}{\partial y}]^T$, is the same as the unit vector along the tangential direction of the desired contour, $[-\frac{f_y}{\sqrt{f_x^2+f_y^2}},\frac{f_x}{\sqrt{f_x^2+f_y^2}}]^T$. It is thus obvious that, in the new TCF, the original contour tracking problem is decoupled into a regulation problem along r_c and a trajectory tracking problem along r_m. Furthermore, around the desired contour, the Jacobian matrix of the curvilinear coordinate transformation (2) can be approximated by

$$\mathbf{J}=\begin{bmatrix} \frac{\partial r_c}{\partial x} & \frac{\partial r_c}{\partial y} \\ \frac{\partial r_m}{\partial x} & \frac{\partial r_m}{\partial y} \end{bmatrix}\approx\begin{bmatrix} \frac{f_x}{\sqrt{f_x^2+f_y^2}} & \frac{f_y}{\sqrt{f_x^2+f_y^2}} \\ -\frac{f_y}{\sqrt{f_x^2+f_y^2}} & \frac{f_x}{\sqrt{f_x^2+f_y^2}} \end{bmatrix} \tag{3}$$

which is unitary for all values of x,y, i.e., $\mathbf{J^{-1}}=\mathbf{J^T}$.

B. System Dynamics

The dynamics of the biaxial linear-motor-driven gantry can be described by [9]:

$$\mathbf{M}\ddot{\mathbf{q}}+\mathbf{B}\dot{\mathbf{q}}+\mathbf{F}(\dot{\mathbf{q}})=\mathbf{u}+\mathbf{d} \tag{4}$$

where $\mathbf{M}=diag[M_1,M_2]$ and $\mathbf{B}=diag[B_1,B_2]$ are the 2×2 diagonal inertia and damping matrices, respectively; $\mathbf{u}$ is the 2×1 vector of control input, and $\mathbf{d}$ is the 2×1 vector of unknown nonlinear functions due to external disturbances or modeling errors; $\mathbf{F}(\dot{\mathbf{q}})$ is the 2×1 vector of nonlinear friction, and the model used in this paper is given by $\bar{\mathbf{F}}(\dot{\mathbf{q}})=\mathbf{A}\mathbf{S_f}(\dot{\mathbf{q}})$, where $\mathbf{A}=diag[A_1,A_2]$ is the 2×2 diagonal friction coefficient matrix, and $\mathbf{S_f}(\cdot)$ is a vector-valued smooth function, i.e., $\mathbf{S_f}(\dot{\mathbf{q}})=[S_f(\dot{x}),S_f(\dot{y})]^T$. Define the approximation error as $\widetilde{\mathbf{F}}=\bar{\mathbf{F}}-\mathbf{F}$. Then (4) can be written as

$$\mathbf{M}\ddot{\mathbf{q}}+\mathbf{B}\dot{\mathbf{q}}+\mathbf{A}\mathbf{S_f}(\dot{\mathbf{q}})=\mathbf{u}+\mathbf{d_n}+\widetilde{\mathbf{d}} \tag{5}$$

where $\mathbf{d_n}=[d_{n1},d_{n2}]^T$ is the nominal value of $\mathbf{d_1}=\mathbf{d}+\widetilde{\mathbf{F}}$, and $\widetilde{\mathbf{d}}=\mathbf{d_1}-\mathbf{d_n}$. Noting (2) and (3), $\dot{\mathbf{r}}=\mathbf{J}\dot{\mathbf{q}}(t),\ddot{\mathbf{r}}=\mathbf{J}\ddot{\mathbf{q}}(t)+\dot{\mathbf{J}}\dot{\mathbf{q}}(t)$. Thus (5) can be transformed into the global TCF as

$$\mathbf{M_t}\ddot{\mathbf{r}}+\mathbf{B_t}\dot{\mathbf{r}}+\mathbf{C_t}\dot{\mathbf{r}}+\mathbf{A_t}\mathbf{S_f}(\dot{\mathbf{q}})=\mathbf{u_t}+\mathbf{d_t}+\widetilde{\Delta} \tag{6}$$

where $\mathbf{M_t}=\mathbf{J}\mathbf{M}\mathbf{J}^{-1}$, $\mathbf{B_t}=\mathbf{J}\mathbf{B}\mathbf{J}^{-1}$, $\mathbf{C_t}=-\mathbf{J}\mathbf{M}\mathbf{J}^{-1}\dot{\mathbf{J}}\mathbf{J}^{-1}$, $\mathbf{A_t}=\mathbf{J}\mathbf{A}$, $\mathbf{d_t}=\mathbf{J}\mathbf{d_n}$, $\mathbf{u_t}=\mathbf{J}\mathbf{u}$, $\widetilde{\Delta}=\mathbf{J}\widetilde{\mathbf{d}}$. It is well known that equation (6) has several properties [12]: (**P1**) $\mathbf{M_t}$ is a symmetric positive definite (s.p.d.) matrix with $\mu_1\mathbf{I}\le\mathbf{M_t}\le\mu_2\mathbf{I}$ where μ_1 and μ_2 are two positive scalars; (**P2**) The matrix $\mathbf{N_t}=\dot{\mathbf{M}}_\mathbf{t}-2\mathbf{C_t}$ is a skew-symmetric matrix. In other words, $\mathbf{s^T}\mathbf{N_t}\mathbf{s}=0,\forall\mathbf{s}$; (**P3**) $\mathbf{M_t}$, $\mathbf{B_t}$, $\mathbf{C_t}$, $\mathbf{A_t}$, $\mathbf{d_t}$ and $\mathbf{u_t}$ in (6) can be linearly parameterized by a set of unknown parameters defined as $\theta=[\theta_1,...,\theta_8]^T=[M_1,M_2,B_1,B_2,A_1,A_2,d_{n1},d_{n2}]^T$.

Assumption 1: Extent of parametric uncertainties and uncertain nonlinearities is known. More precisely,

$$\begin{aligned}\theta\in\Omega_\theta&\triangleq\{\theta:\ \theta_{min}\le\theta\le\theta_{max}\}\\ \widetilde{\Delta}\in\Omega_\Delta&\triangleq\left\{\widetilde{\Delta}:\ ||\widetilde{\Delta}||\le\delta_\Delta\right\}\end{aligned} \tag{7}$$

where $\theta_{min}=[\theta_{1min},...,\theta_{8min}]^T$, and $\theta_{max}=[\theta_{1max},...,\theta_{8max}]^T$ are known constant vectors and δ_Δ is a known function.

The control objective is to synthesize a control input $\mathbf{u_t}$ such that $\mathbf{q}=[x,y]^T$ tracks $\mathbf{q_d}(t)=[x_d,y_d]^T$ which is at least second-order differentiable. In the proposed global TCF, such an objective is achieved simply by regulating r_c to zero and letting r_m follow $r_{md}(t)=r_m(x_d(t),y_d(t))$.

III. Integrated Direct/Indirect Adaptive Robust Contouring Control (DIARC)

A. Projection Type Adaptation Law

Let $\widehat{\theta}$ denote the estimate of θ and $\widetilde{\theta}$ denote the estimation error (i.e., $\widetilde{\theta} = \widehat{\theta} - \theta$). By (7), the following projection type adaptation law can be used

$$\dot{\widehat{\theta}} = Proj_{\widehat{\theta}}(\Gamma\tau) \tag{8}$$

where Γ is a positive definite matrix, τ is an adaptation function to be synthesized later. The standard projection mapping $Proj_{\widehat{\theta}}(\bullet) = [Proj_{\widehat{\theta}_1}(\bullet_1), ..., Proj_{\widehat{\theta}_8}(\bullet_8)]^T$ in [14] should be used to keep the parameter estimates $\widehat{\theta}_1, ..., \widehat{\theta}_8$ within the known bound. And it is easy to show that the projection type adaptation law (8) in which $\Gamma(t) > 0$ is any continuously differentiable positive definite symmetric adaptation rate matrix has the following properties [14]:

$$\begin{aligned} &\textbf{(P4)}.\ \widehat{\theta} \in \Omega_\theta \triangleq \left\{\widehat{\theta} : \theta_{imin} \le \widehat{\theta} \le \theta_{imax}\right\} \\ &\textbf{(P5)}.\ \widetilde{\theta}^T(\Gamma^{-1}\mathrm{Proj}_{\widehat{\theta}}(\Gamma\tau) - \tau) \le 0,\ \forall\tau \end{aligned} \tag{9}$$

B. Integrated DIARC Contouring Control Law Synthesis

Define a switching-function-like quantity as $\mathbf{s} = \dot{\mathbf{e}} + \Lambda\mathbf{e} = \dot{\mathbf{r}} - \dot{\mathbf{r}}_{\mathbf{eq}}, \dot{\mathbf{r}}_{\mathbf{eq}} \triangleq \dot{\mathbf{r}}_{\mathbf{d}} - \Lambda\mathbf{e}$ where $\mathbf{e} = \mathbf{r(t)} - \mathbf{r_d(t)}$ is the output tracking error, and $\Lambda > 0$ is a diagonal matrix. Define a positive semi-definite (p.s.d.) function

$$V(t) = \tfrac{1}{2}\mathbf{s^T M_t(r)s} \tag{10}$$

Differentiating V yields

$$\dot{V}(t) = \mathbf{s^T}[\mathbf{u_t} - \mathbf{M_t}\ddot{\mathbf{r}}_{\mathbf{eq}} - \mathbf{B_t}\dot{\mathbf{r}} - \mathbf{C_t}\dot{\mathbf{r}}_{\mathbf{eq}} - \mathbf{A_t S_f}(\dot{\mathbf{q}}) + \mathbf{d_t} + \widetilde{\Delta}] \tag{11}$$

where $\ddot{\mathbf{r}}_{\mathbf{eq}} \triangleq \ddot{\mathbf{r}}_{\mathbf{d}} - \Lambda\dot{\mathbf{e}}$, and (P2) is used to eliminate the term $\frac{1}{2}\mathbf{s^T}\dot{\mathbf{M}}_{\mathbf{t}}(\mathbf{r})\mathbf{s}$. Furthermore, since it follows from (P3) that $\mathbf{M_t}\ddot{\mathbf{r}}_{\mathbf{eq}} + \mathbf{B_t}\dot{\mathbf{r}} + \mathbf{C_t}\dot{\mathbf{r}}_{\mathbf{eq}} + \mathbf{A_t S_f}(\dot{\mathbf{q}}) - \mathbf{d_t} = -\Psi(\mathbf{r}, \dot{\mathbf{r}}, \dot{\mathbf{r}}_{\mathbf{eq}}, \ddot{\mathbf{r}}_{\mathbf{eq}})\theta$ where $\Psi(\mathbf{r}, \dot{\mathbf{r}}, \dot{\mathbf{r}}_{\mathbf{eq}}, \ddot{\mathbf{r}}_{\mathbf{eq}})$ is a 2×8 matrix of known functions, commonly referred to as the *regressor*. Thus, from (11),

$$\dot{V}(t) = \mathbf{s^T}[\mathbf{u_t} + \Psi(\mathbf{r}, \dot{\mathbf{r}}, \dot{\mathbf{r}}_{\mathbf{eq}}, \ddot{\mathbf{r}}_{\mathbf{eq}})\theta + \widetilde{\Delta}] \tag{12}$$

Noting (12), the following DIARC law is proposed:

$$\begin{aligned} &\mathbf{u_t} = \mathbf{u_a} + \mathbf{u_s},\ \mathbf{u_a} = \mathbf{u_{a1}} + \mathbf{u_{a2}},\ \mathbf{u_s} = \mathbf{u_{s1}} + \mathbf{u_{s2}}, \\ &\mathbf{u_{a1}} = -\Psi(\mathbf{r}, \dot{\mathbf{r}}, \dot{\mathbf{r}}_{\mathbf{eq}}, \ddot{\mathbf{r}}_{\mathbf{eq}})\widehat{\theta},\ \mathbf{u_{s1}} = -\mathbf{Ks} \end{aligned} \tag{13}$$

where $\mathbf{u_{a1}}$ is the adjustable model compensation needed for achieving perfect tracking with $\widehat{\theta}$ being the on-line estimates of physical parameters to be detailed later, $\mathbf{u_{a2}}$ is a fast dynamic compensation term to be synthesized in the following, $\mathbf{u_{s1}}$ is used to stabilize the nominal system, which is chosen to be a simple proportional feedback with $\mathbf{K}$ being a symmetric positive definite matrix for simplicity. And $\mathbf{u_{s2}}$ is a feedback used to attenuate the effect of model uncertainties for a guaranteed robust performance. Substituting (13) into (12) and simplifying the resulting expression lead to

$$\dot{V} = \mathbf{s^T}[\mathbf{u_{a2}} + \mathbf{u_s} - \Psi(\mathbf{r}, \dot{\mathbf{r}}, \dot{\mathbf{r}}_{\mathbf{eq}}, \ddot{\mathbf{r}}_{\mathbf{eq}})\widetilde{\theta} + \widetilde{\Delta}] \tag{14}$$

Define a constant $\mathbf{d_c}$ and time varying function $\widetilde{\mathbf{d}}^*(t)$ as

$$\mathbf{Jd_c} + \widetilde{\mathbf{d}}^*(t) = -\Psi(\mathbf{r}, \dot{\mathbf{r}}, \dot{\mathbf{r}}_{\mathbf{eq}}, \ddot{\mathbf{r}}_{\mathbf{eq}})\widetilde{\theta} + \widetilde{\Delta} \tag{15}$$

Conceptually, (15) lumps the disturbance and the model uncertainties due to parameter estimation error together, and divides it into the low frequency component $\mathbf{d_c}$ and the higher frequency components $\widetilde{\mathbf{d}}^*(t)$, so that $\mathbf{d_c}$ can be compensated through the fast adaptation of direct adaptive robust control (DARC) design [11]. Substituting (15) into (14),

$$\dot{V} = \mathbf{s^T}[\mathbf{u_{a2}} + \mathbf{u_s} + \mathbf{Jd_c} + \widetilde{\mathbf{d}}^*(t)] \tag{16}$$

Choose the fast compensation term $\mathbf{u_{a2}}$ as

$$\mathbf{u_{a2}} = -\mathbf{J}\widehat{\mathbf{d_c}} \tag{17}$$

where $\widehat{\mathbf{d_c}}$ represents the estimate of $\mathbf{d_c}$ updated by

$$\dot{\widehat{\mathbf{d}}}_{\mathbf{c}} = Proj_{\widehat{\mathbf{d}}_{\mathbf{c}}}(\gamma_{\mathbf{d}}\mathbf{J^T s}), \qquad |\widehat{\mathbf{d}}_{\mathbf{c}}(\mathbf{0})| \le \widehat{\mathbf{d}}_{\mathbf{c}max} \tag{18}$$

where $\widehat{\mathbf{d}}_{\mathbf{c}max}$ is a pre-set bound for $\widehat{\mathbf{d}}_{\mathbf{c}}(t)$ and $\gamma_{\mathbf{d}}$ is a 2×2 constant diagonal matrix. By (9), the projection mapping in (18) guarantees $|\widehat{\mathbf{d}}_{\mathbf{c}}(t)| \le \widehat{\mathbf{d}}_{\mathbf{c}max}, \forall t$. Substituting (17) into (16),

$$\dot{V} = \mathbf{s^T}[-\mathbf{Ks} + \mathbf{u_{s2}} - \mathbf{J}\widetilde{\mathbf{d}}_{\mathbf{c}} + \widetilde{\mathbf{d}}^*(t)] \tag{19}$$

where $\mathbf{u_{s2}}$ is chosen to satisfy the following two conditions:

$$\begin{aligned} &i \qquad \mathbf{s^T}[\mathbf{u_{s2}} - \mathbf{J}\widetilde{\mathbf{d}}_{\mathbf{c}} + \widetilde{\mathbf{d}}^*(t)] \le \quad \eta \\ &ii \qquad \mathbf{s^T u_{s2}} \le \mathbf{0} \end{aligned} \tag{20}$$

where η is a constant that can be arbitrarily small. One smooth example of $\mathbf{u_{s2}}$ satisfying (20) is $\mathbf{u_{s2}} = -\frac{1}{4\eta}h^2\mathbf{s}$, where h is a smooth function satisfying $h \ge ||\widehat{\mathbf{d}}_{\mathbf{c}max}|| + ||\theta_{\mathbf{M}}||||\Psi(\mathbf{r}, \dot{\mathbf{r}}, \dot{\mathbf{r}}_{\mathbf{eq}}, \ddot{\mathbf{r}}_{\mathbf{eq}})|| + \delta_\Delta$, and $\theta_{\mathbf{M}} = \theta_{max} - \theta_{min}$.

Theorem 1: With the DIARC control law (13) and the projection type adaptation law (8), regardless the estimation function τ to be used, in general, all signals in the resulting closed loop system are bounded and the contouring error and output position tracking error are guaranteed to have a prescribed transient performance and steady-state accuracy in the sense that $V(t)$ defined by (10) is bounded by

$$V(t) \le exp(-\lambda t)V(0) + \tfrac{\eta}{\lambda}[1 - exp(-\lambda t)] \tag{21}$$

where $\lambda = 2\sigma_{min}(\mathbf{K})/\mu_2$, and $\sigma_{min}(\cdot)$ denotes the minimum eigenvalue of a matrix.

C. Estimation of Physical Parameters

This subsection focuses on the construction of suitable estimation functions τ so that an improved steady-state performance – zero steady-state contouring error and position tracking error – can be obtained even when all physical parameters are unknown. In addition, it is desirable to have on-line parameter estimates converge or stay close to their true values for other purposes such as machine health monitoring. To this end, in this subsection, it is assumed that system has parametric uncertainties only, i.e., $\widetilde{\mathbf{d}} = 0$ in (5).

Let $H_f(s)$ be the transfer function of any filter with a relative degree not less than 1 (e.g., $H_f(s) = 1/(\tau_f s + 1)$). Then, applying the filter to both sides of (5), when $\widetilde{\mathbf{d}} = 0$,

$$\mathbf{u_f} = \Upsilon_{\mathbf{f}}^{\mathbf{T}}\theta \tag{22}$$

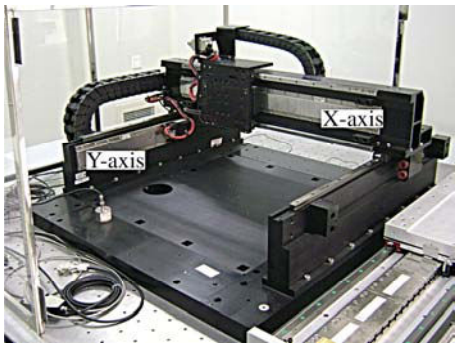

Fig. 2. A biaxial linear-motor-driven gantry system.

where $\mathbf{u_f} = \begin{bmatrix} u_{1f} \\ u_{2f} \end{bmatrix}$, $\Upsilon_\mathbf{f}^\mathbf{T} = \begin{bmatrix} \ddot{x}_f, 0, \dot{x}_f, 0, S_{ff}(\dot{x}), 0, 1_f, 0 \\ 0, \ddot{y}_f, 0, \dot{y}_f, 0, S_{ff}(\dot{y}), 0, 1_f \end{bmatrix}$, and $\bullet_f$ represents the filtered value of $\bullet$. Define the prediction error vector as $\varsigma = \widehat{\mathbf{u}}_\mathbf{f} - \mathbf{u_f}$, where $\widehat{\mathbf{u}}_\mathbf{f} = \Upsilon_\mathbf{f}^\mathbf{T}\widehat{\theta}$. Then,

$$\varsigma = \Upsilon_\mathbf{f}^\mathbf{T}\widetilde{\theta} = \Upsilon_\mathbf{f}^\mathbf{T}\widehat{\theta} - \mathbf{u_f} \tag{23}$$

This linear regression model (23) is the standard form to which various parameter estimation algorithms can be applied for the estimates of θ. For example, with the least squares type estimation algorithm [12], $\widehat{\theta}$ is updated by the adaptation law (8) with the adaptation function given by

$$\tau = -\frac{1}{1 + \upsilon tr\{\Upsilon_\mathbf{f}^\mathbf{T}\Gamma\Upsilon_\mathbf{f}\}}\Upsilon_\mathbf{f}\varsigma \tag{24}$$

and the adaptation rate matrix given by

$$\dot{\Gamma} = \begin{cases} \kappa\Gamma - \frac{1}{1+\upsilon tr\{\Upsilon_\mathbf{f}^\mathbf{T}\Gamma\Upsilon_\mathbf{f}\}}\Gamma\Upsilon_\mathbf{f}\Upsilon_\mathbf{f}^\mathbf{T}\Gamma, \text{if } \lambda_{max}(\Gamma(t)) \le \rho_M \\ 0, \text{ otherwise} \end{cases} \tag{25}$$

where $\kappa \ge 0$ is the forgetting factor, ρ_M is the pre-set upper bound for $\|\Gamma(t)\|$, $\upsilon \ge 0$ with $\upsilon = 0$ leading to the unnormalized algorithm. With these practical modifications, $\Gamma(t) \le \rho_M I$, $\forall t$. Furthermore, it can be shown that if the following persistent excitation (PE) condition is satisfied:

$$\int_t^{t+T} \Upsilon_\mathbf{f}\Upsilon_\mathbf{f}^\mathbf{T} d\tau \ge \kappa_p I_p, \text{ for some } \kappa_p > 0 \text{ and } T > 0 \tag{26}$$

then, the physical parameter estimate $\widehat{\theta}$ converge to their true values (i.e., $\widetilde{\theta} \to 0$ as $t \to \infty$) and $\widetilde{\theta} \in L_2[0,\infty)$.

Theorem 2: If after a finite time t_0 there exist parametric uncertainties only, i.e., $\widetilde{\mathbf{d}} = 0$, $\forall t \ge t_0$ in (5), by using the DIARC control law (13) and the projection type adaption law (8) with the least squares type estimation function (24), if the PE condition (26) is satisfied, in addition to the robust performance results stated in Theorem 1, an improved final contouring performance – asymptotic output contouring – is also achieved, i.e. $\varepsilon_c \to 0$ and $\mathbf{s} \to 0$ as $t \to \infty$.

IV. Experimental Setup and Results

A. Experimental setup

As shown in Fig. 2, the same biaxial industrial gantry from Rockwell Automation as in [8], [9] is used as a test-bed. The two axes powered by Anorad LC-50-200 iron core linear motors are mounted orthogonally with X-axis on top of Y-axis. The position sensors of the gantry are two linear encoders with a resolution of $0.5\mu m$ after quadrature. The velocity signal is obtained by the difference of two consecutive position measurements. Standard least-square identification is performed to obtain the parameters of the biaxial gantry and it is found that nominal values of the gantry system parameters without loads are $M_1 = 0.12V/m/s^2, M_2 = 0.55V/m/s^2, B_1 = 0.35V/m/s, B_2 = 0.5V/m/s, A_{f1} = 0.1V, A_{f2} = 0.13V, d_{N1} = 0V, d_{N2} = 0V$ which is different from our previous publications because the physical characteristic of the gantry have changed due to the long past time and some added lubricant. The bounds of the parametric variations are chosen as $\theta_{min} = [0.06, 0.4, 0.2, 0.3, 0.05, 0.08, -0.5, -0.5]^T$ and $\theta_{max} = [0.25, 0.7, 0.6, 0.6, 0.15, 0.25, 0.5, 0.5]^T$.

As in [8], the performance indexes $||\varepsilon_c||_{rms}$, the root-mean-square (RMS) value of the contouring error, ε_{cM}, the maximum absolute value of the contouring error, and $||u_i||_{rms}$, the average control input, will be used to measure the quality of each control algorithm quantitatively.

B. Contouring experimental results

The control algorithms are implemented using a dSPACE DS1103 controller board. The controller executes programs at a sampling period of $T_s = 0.2ms$, resulting in a velocity measurement resolution of $0.0025m/s$. The following three control algorithms are implemented and compared:

C1: Global TCF based DARC – the same GTCF but with the DARC contouring control law synthesized as in [8]. $S_f(\dot{x}) = \frac{2}{\pi}arctan(9000\dot{x})$, $S_f(\dot{y}) = \frac{2}{\pi}arctan(9000\dot{y})$, and $\Lambda = diag[100, 30]$. In implementation, a large enough constant feedback gain is used to simplify the resulting control law $\mathbf{u_{s2}}$, with the total feedback gain in (13) chosen as $\mathbf{K} = diag[100, 60]$. The adaptation rates are $\Gamma = diag[10, 10, 10, 10, 10, 10, 10000, 10000]$. The initial parameter estimates are $\widehat{\theta}(0) = [0.1, 0.55, 0.3, 0.3, 0.1, 0.15, 0, 0]^T$.

C2: Global TCF based DIARC control law proposed in Section III. The same $S_f(\dot{x})$, $S_f(\dot{y})$, Λ, $\mathbf{u_{s2}}$, and $\mathbf{K} = diag[100, 60]$ as in C1 are used. In (18), $\widehat{\mathbf{d}}_{\mathbf{c}max} = [1, 1]^T$ and $\gamma_\mathbf{d} = diag[10000, 10000]$. The filter $H_f(s)$ is chosen to be of second-order with a relative degree of 2 and damping ratio of 0.7, with the break frequencies of 250Hz and 150Hz for X-axis and Y-axis, respectively. In (25), κ=0.1, υ=0.1. $\Gamma(0) = diag[10, 10, 10, 10, 10, 10, 5000, 5000]$ and $\rho_M = 500$. The initial parameter estimates are the same as those in C1.

C3: Local TCF based DIARC detailed in [12]. The control parameters are chosen the same as in C2.

The following three test sets are performed:

Set1: To test the nominal contouring performance of the controllers, experiments are run without payload, which is equivalent to $M_1 = 0.12$ and $M_2 = 0.55$;

Set2: To test the performance robustness of the algorithms to parameter variations, a 5 kg payload is mounted on the gantry, which is equivalent to $M_1 = 0.19$ and $M_2 = 0.62$;

Set3: A large step disturbance (a simulated 0.6 V electrical signal) is added to the input of Y axis at t=2.2 sec and removed at t=5.2 sec to test the performance robustness of each controller to disturbance.

TABLE I

CONTOURING RESULTS OF EXPERIMENTS I

	$\|\|\varepsilon_c\|\|_{rms}(\mu m)$	$\varepsilon_{cM}(\mu m)$	$\|\|u_x\|\|_{rms}(V)$	$\|\|u_y\|\|_{rms}(V)$
C1 (Set1)	2.42	8.57	0.42	0.70
C2 (Set1)	2.42	8.15	0.42	0.68
C3 (Set1)	3.30	10.14	0.41	0.70
C1 (Set2)	2.50	9.52	0.54	0.78
C2 (Set2)	2.44	8.38	0.54	0.78
C3 (Set2)	3.38	10.21	0.54	0.78
C1 (Set3)	2.73	37.48	0.42	0.75
C2 (Set3)	2.73	36.52	0.42	0.74
C3 (Set3)	3.54	36.54	0.42	0.75

TABLE II

CONTOURING RESULTS OF EXPERIMENTS II

	$\|\|\varepsilon_c\|\|_{rms}(\mu m)$	$\varepsilon_{cM}(\mu m)$	$\|\|u_x\|\|_{rms}(V)$	$\|\|u_y\|\|_{rms}(V)$
C1 (Set1)	2.57	8.72	0.33	0.62
C2 (Set1)	2.60	9.64	0.33	0.61
C3 (Set1)	4.15	13.98	0.32	0.61
C1 (Set2)	2.74	9.93	0.38	0.66
C2 (Set2)	2.74	9.74	0.38	0.67
C3 (Set2)	4.19	15.72	0.38	0.68
C1 (Set3)	2.91	36.10	0.33	0.68
C2 (Set3)	2.93	35.30	0.33	0.67
C3 (Set3)	4.40	38.51	0.32	0.68

1) Experiments I: The biaxial gantry is first commanded to track an ellipse of $\mathbf{q_d} = [0.2sin(4t), -0.1cos(4t) + 0.1]^T$ with an angular velocity of $w = 4rad/s$ and a speed of $v = \sqrt{0.16 + 0.48cos^2(4t)}m/s$. The experimental results after running the gantry for several periods are given in Table I – both C1 and C2 achieve good steady-state contouring performances during fast elliptical movements, while C1 and C2 performs better than C3 with almost the same amount of control efforts for every test set. Furthermore, the steady-state contouring errors of C2 for Set2 are almost the same as those for Set1, validating the strong performance robustness of the proposed controller to the change of inertia load. The desired contour and the actual contours of three controllers for all sets are partially shown in Fig.3 around $(0.2m, 0.1m)$ where the ellipse has the largest curvature. It can be seen that, for all sets, the actual contours of C1 and C2 are quite close to the desired contours, while the actual contours of C3 deviate from the desired contour significantly. These results clearly demonstrate the superiority of the proposed global TCF used in C1 and C2 over the traditional local TCF in C3 when dealing with contours of large curvatures.

2) Experiments II: To test the consistency of the proposed algorithms, the gantry is also commanded to track another ellipse given by $\mathbf{q_d} = [0.2sin(3t), -0.15cos(3t) + 0.15]^T$ with an angular velocity of $\omega = 3rad/s$ and a speed of $v = \sqrt{0.2025 + 0.1575cos^2(3t)}m/s$. The experimental results in Table II show the same trends as in Experiments I – the better contouring performance of C1 and C2 over C3 with almost the same amount of control efforts. The time-histories of contouring errors for Set2 are displayed in Fig.4, showing that C2 achieves excellent steady-state contouring performance in spite of the change of inertia load. It is worth noting that the contouring error of C3 appears to have a constant negative offset, which is due to the fact that the contouring error in C3 is approximately calculated based on the projection of the actual tracking errors in the LTCF. The contouring error shown in Fig.5 also shows that the added large disturbances do not affect the contouring performance of the proposed algorithms much except the initial transient when the sudden changes of the disturbances occur. The desired contours and the actual contours of all controllers for all sets are partially shown in Fig.6 around $(-0.2m, 0.15m)$. It is seen again that the actual contours of C1 and C2 in all sets are much more closer to the desired contours than those of C3.

C. Parameter Estimation Results

While achieving excellent contouring performance, the proposed C2 also achieves good parameter estimations which cannot be achieved by C1. Fig.7 shows the histories of parameter estimations of X-axis for C2 and C3 for no-load experiments. As seen, regardless of the ellipses to be tracked (i.e., experiments I or II), the parameter estimates of both DIARC controllers (i.e., C2 and C3) consistently approach the off-line estimated values without payload. The results shown in Fig.8 for loaded situation also show that the on-line parameter estimates of Y-axis for C2 and C3, approach to the off-line estimated values with the payload. In summary, the proposed global TCF based DIARC strategy possesses the merits of both the global TCF based DARC and the local TCF based DIARC – excellent contouring performance and accurate on-line parameter estimations.

V. CONCLUSIONS

In this paper, a global task coordinate frame (GTCF) based integrated direct/indirect adaptive robust controller (DIARC) is synthesized for the coordinated motion control of biaxial systems. The GTCF used in the paper provides a rather straightforward and accurate calculation of contouring errors, overcoming the inability of the existing locally defined moving TCF in dealing with contours having large curvature or large tracking errors. The parameter adaptation law of DIARC enables estimation algorithms having good convergence properties such as the least-squares type and explicit on-line monitoring of signal excitation levels to be used for accurate parameter estimations. Comparative experimental results reveal that the proposed GTCF based DIARC algorithm not only achieves excellent contouring performance for high-speed/large-curvature contouring applications but also has accurate parameter estimations in practical applications.

REFERENCES

[1] M.-Y. Cheng and C.-C. Lee, "Motion controller design for contour-following tasks based on real-time contour error estimation," *IEEE Trans. on Indus. Elect.*, vol. 54, no. 3, pp. 1686–1695, June 2007.

[2] S.-L. Chen and K.-C. Wu, "Contouring control of smooth paths for multi-axis motion systems based on equivalent errors," *IEEE Trans. on Cont. Syst. Tech.*, vol. 15, no. 6, pp. 1151–1158, Nov. 2007.

[3] J. Yang and Z. Li, "A novel contour error estimation for position loop-based cross-coupled control," *IEEE/ASME Transactions on Mechatronics*, accepted in 2010 with DOI 10.1109/TMECH.2010.2048718.

[4] Y. Koren, "Cross-coupled biaxial computer control for manufacturing systems," *ASME Journal of Dynamic Systems, Measurement, and Control*, vol. 102, pp. 265–272, 1980.

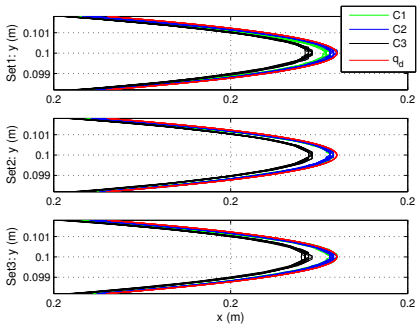

Fig. 3. Partial contours of C1, C2, C3 and desired $\mathbf{q_d}(t)$ for experiments I in all sets.

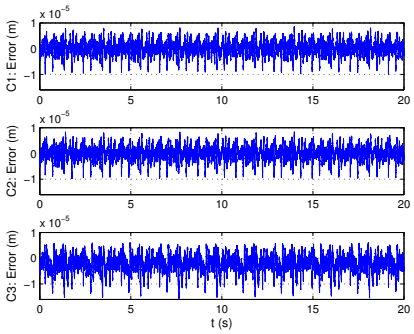

Fig. 4. Contouring errors of C1, C2 and C3 for experiments II at Set2 (loaded).

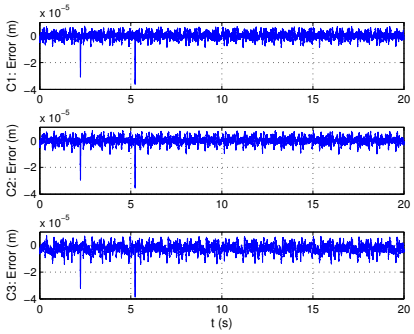

Fig. 5. Contouring errors of C1, C2 and C3 for experiments II at Set3 (with disturbance).

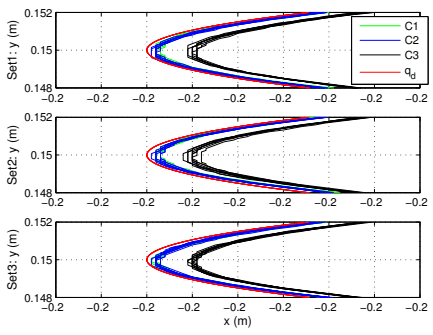

Fig. 6. Partial contours of C1, C2, C3 and desired $\mathbf{q_d}(t)$ for experiments II in all sets.

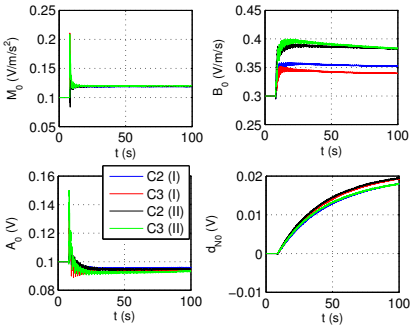

Fig. 7. X-axis parameter estimates of C2 and C3 for experiments I and II at Set1 (no load).

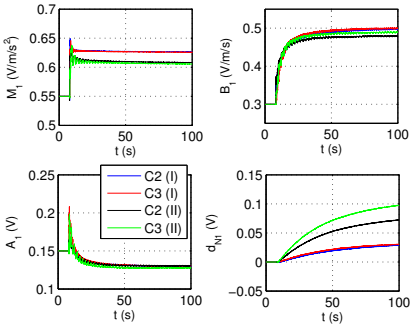

Fig. 8. Y-axis parameter estimates of C2 and C3 for experiments I and II at Set2 (loaded).

[5] B. Yao, S. P. Chan, and D. Wang, "Unified formulation of variable structure control schemes to robot manipulators," *IEEE Trans. on Automatic Control*, vol. 39, no. 2, pp. 371–376, 1994.

[6] G. T.-C. Chiu and M. Tomizuka, "Contouring control of machine tool feed drive systems: A task coordinate frame approach," *IEEE Trans. Control System Technology*, vol. 9, pp. 130–139, Jan. 2001.

[7] C.-L. Chen and K.-C. Lin, "Observer-based contouring controller design of a biaxial stage system subject to friction," *IEEE Trans. on Control System Technology*, vol. 16, no. 2, pp. 322–329, March 2008.

[8] C. Hu, Bin Yao, and Q. Wang, "Coordinated adaptive robust contouring controller design for an industrial biaxial precision gantry," *IEEE/ASME Trans. on Mechatronics*, vol. 15, no. 5, pp.728–735, 2010.

[9] C. Hu, Bin Yao, and Q. Wang, "Coordinated adaptive robust contouring control of an industrial biaxial precision gantry with cogging force compensations," *IEEE Transactions on Industrial Electronics*, vol. 57, no. 5, pp. 1746–1754, May 2010.

[10] Bin Yao, "High performance adaptive robust control of nonlinear systems: a general framework and new schemes," in *Proc. of IEEE Conf. on Decision and Control*, pp. 2489–2494, San Diego, 1997.

[11] B. Yao and M. Tomizuka, "Adaptive robust control of SISO nonlinear systems in a semi-strict feedback form," *Automatica*, vol. 33, no. 5, pp. 893–900, 1997.

[12] C. Hu, Bin Yao, and Q. Wang, "Integrated direct/indirect adaptive robust contouring control of a biaxial gantry with accurate parameter estimations," *Automatica*, vol. 46, no. 4, pp. 701–707, 2010.

[13] Bin Yao, C. Hu, and Q. Wang, "An orthogonal global task coordinate frame for contouring control of biaxial systems," *IEEE/ASME Trans. on Mechatronics*, accepted in 2011 with DOI 10.1109/TMECH.2011.2111377.

[14] B. Yao, "Integrated direct/indirect adaptive robust control of siso nonlinear systems in semi-strict feedback form," in the *American Control Conference*, Denver, USA, Jun. 2003, pp. 3020-3025. O. Hugo Schuck Best Paper Award.